AD-A136 237 MONTE CARLO STUDY OF THE PHASE DIAGRAMS OF BINARY ALLOYS WITH FACE-CENTER..(U) RUTGERS - THE STATE UNIV NEW BRUNSWICK N J DEPT OF MATHEMATIC.. K BINDER ET AL. 1/1

UNCLASSIFIED 1982 AFOSR-TR-83-1017 AFOSR-78-3522 F/G 12/1 NL

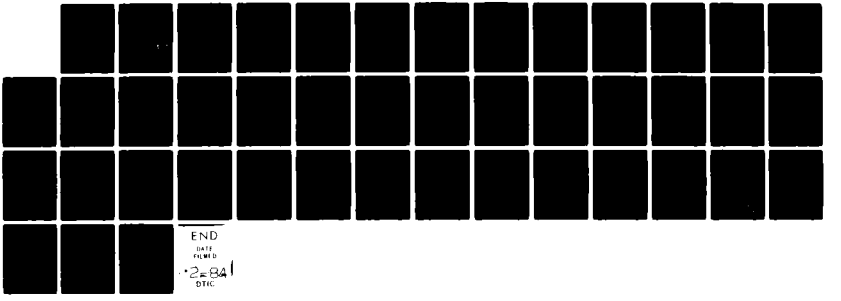

END

DATE FILMED

2-84

DTIC

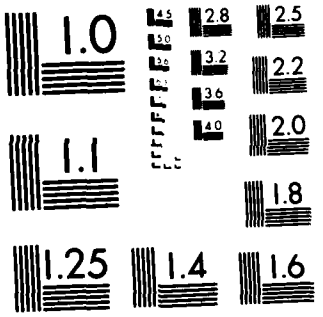

UNCLASSIFIED

SECURITY CLASSIFICATION OF THIS PAGE (When Data Entered)

REPORT DOCUMENTATION PAGE		READ INSTRUCTIONS BEFORE COMPLETING FORM
1. REPORT NUMBER AFOSR-TR- 83-1017	2. GOVT ACCESSION NO.	3. RECIPIENT'S CATALOG NUMBER
4. TITLE (and Subtitle) MONTE CARLO STUDY OF THE PHASE DIAGRAMS OF BINARY ALLOYS WITH FACE-CENTERED CUBIC LATTICE STRUCTURE		5. TYPE OF REPORT & PERIOD COVERED Interim 6. PERFORMING ORG. REPORT NUMBER
7. AUTHOR(s) Kurt Binder, Institut für Festkörperforschung; Joel L. Lebowitz, Mohan K. Phani, Rutgers University; Malvin H. Kalos, Courant Institute of Mathematical Science		8. CONTRACT OR GRANT NUMBER(s) AFOSR -78-3522
9. PERFORMING ORGANIZATION NAME AND ADDRESS Rutgers University Department of Mathematics New Brunswick, New Jersey 08903		10. PROGRAM ELEMENT, PROJECT, TASK AREA & WORK UNIT NUMBERS 61102F 2301/A8
11. CONTROLLING OFFICE NAME AND ADDRESS AFOSR/NP Bolling AFB, Bldg. #410 Washington, D.C. 20332		12. REPORT DATE 1982 13. NUMBER OF PAGES 41
14. MONITORING AGENCY NAME & ADDRESS(if different from Controlling Office)		15. SECURITY CLASS. (of this report) Unclassified 15a. DECLASSIFICATION/DOWNGRADING SCHEDULE

16. DISTRIBUTION STATEMENT (of this Report)

Approved for public release; distribution unlimited

17. DISTRIBUTION STATEMENT (of the abstract entered in Block 20, if different from Report)

18. SUPPLEMENTARY NOTES

19. KEY WORDS (Continue on reverse side if necessary and identify by block number)

Monte Carlo computations; binary alloys; phase diagram; nearest neighbor interaction

20. ABSTRACT (Continue on reverse side if necessary and identify by block number)

We describe the results of Monte Carlo computations of the coherent phase diagram (in the temperature-composition plane) of ordering binary alloys on a face-centered cubic lattice. Results on long- and short-range order parameters as well as ordering energies are also given. We consider the system with nearest neighbor interaction in the grand-canonical ensemble (equivalent to an Ising antiferromagnet in a magnetic field) as well as in the canonical ensemble (fixed composition. Results with next-nearest neighbor

DD FORM 1 JAN 73 1473 EDITION OF 1 NOV 65 IS OBSOLETE

UNCLASSIFIED

SECURITY CLASSIFICATION OF THIS PAGE (When Data Entered)

20. Abstract (continued)

interaction are also given, and for both models a comparison with other available predictions is made, particularly with the cluster-variation method. While the latter is found to be quite accurate at stoichiometric composition, it appears to do less well in the more general case. The tetrahedral approximation of the cluster variation method predicts a topology of the phase diagram, in the case of nearest-neighbor interaction different from the computer simulations. Some consequences for the interpretation of the behavior of copper-gold alloys are indicated.

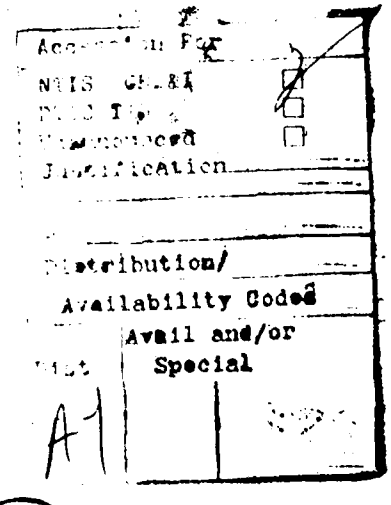

Monte Carlo Study of the Phase Diagrams of Binary Alloys with Face-Centered Cubic Lattice Structure*

by

Kurt Binder

Institut für Festkörperforschung, Kernforschungsanlage Jülich, D-5170 Jülich, Postfach 1913, West-Germany

and

Joel L. Lebowitz and Mohan K. Phani+

Department of Mathematics and Physics, Rutgers University, New Brunswick, N.J. 08903, USA

and

Malvin H. Kalos

Courant Institute of Mathematical Science, New York University, 251 Mercer Street, New York, N.Y. 10012, USA

Abstract:

We describe the results of Monte Carlo computations of the coherent phase diagram (in the temperature-composition plane) of ordering binary alloys on a face-centered cubic lattice. Results on long- and short-range order parameters as well as ordering energies are also given. We consider the system with nearest neighbor interaction in the grand-canonical ensemble (equivalent to an Ising antiferromagnet in a magnetic field) as well as in the canonical ensemble (fixed composition). The close agreement between both approaches serves as a severe test of the good accuracy obtained, and so does the fact that differences between results for lattices with 2048 sites and with 16384 sites are found to be negligibly small. Results with next-nearest neighbor interaction are also given, and for both models a comparison with other available predictions is made, particularly with the cluster-variation method. While the latter is found to be quite accurate at stoi-

chiometric composition, it appears to do less well in the more general case. The tetrahedral approximation of the cluster variation method predicts a topology of the phase diagram, in the case of nearest-neighbor interaction different from the computer simulations. Some consequences for the interpretation of the behavior of copper-gold alloys are indicated.

*Supported in part by ~~AFSOR~~ AFOSR Grant No. ~~78-3522~~ AFOSR-78-3522 and in part by Applied Mathematics Research Program under Contract No. DE-AC02-76ER03077 with the US Department of Energy.

+Present address: Tata Institute of Fundamental Research, Homi Bhabha Road, Bombay 400005, India.

1. Introduction

We have investigated the behavior of ordering binary alloys such as the copper-gold system on a rigid face-centered cubic (fcc) lattice, within the framework of the Ising-model for binary alloys (AB) where one assumes pairwise interactions between the atoms. Let us denote the local concentration at lattice site i by c_i: $c_i=0$ if it is occupied by an A-atom, $c_i=1$ if it is occupied by a B-atom, and denote the interaction energy of AA-, BB- and AB pairs as v_{ij}^{AA}, v_{ij}^{BB} and v_{ij}^{AB}, respectively. Disregarding vacancies or any other lattice defects the energy of the system is then given by

$$V = \sum_{i\neq j} \{(1-c_i)(1-c_j)v_{ij}^{AA}+[c_i(1-c_j)+c_j(1-c_i)]v_{ij}^{AB}+c_ic_jv_{ij}^{BB}\} , \qquad (1)$$

the sums in Eq. (1) are taken over all pairs of neighbors once. As is well known, for the ordering behavior of this system it is only the ordering energy $(v_{ij}^{AA}+v_{ij}^{BB}-2v_{ij}^{AB})$ which matters, and not the three energies v_{ij}^{AA}, v_{ij}^{BB}, v_{ij}^{AB} separately /1/. This fact is utilized by transforming Eq. (1) to the equivalent problem of an Ising magnet in a magnetic field: a "spin up" ("spin down") at a site i, $S_i=+1(-1)$ can be identified with an A(B) atom at that site, by using $S_i=1-2c_i$. The Ising hamiltonian is then expressed in terms of a spin-spin interaction $J_{ij}=-(v_{ij}^{AA}+v_{ij}^{BB}-2v_{ij}^{AB})/4$ and a magnetic field $H=\frac{1}{2}\sum_{j(\neq i)}(v_{ij}^{AA}-v_{ij}^{BB})+\frac{1}{2}(\mu_A-\mu_B)$, where μ_A and μ_B are the chemical potentials of the A and B atoms:

$$\mathcal{H} = -\sum_{i\neq j} J_{ij}S_iS_j - H\sum_i S_i . \qquad (2)$$

Clearly, for general range of the interaction J_{ij} the description of the ordering behavior of the model described by Eq. (2) is a

formidable problem. Hence we restrict the range of the interaction J_{ij} to nearest and next nearest neighbors on the lattice, as is usually assumed /2-4/. Denoting nearest neighbor and next-nearest neighbor pairs by <nn> and <nnn>, respectively, we have

$$\mathcal{H} = -J \sum_{<nn>} S_i S_j + \alpha J \sum_{<nnn>} S_i S_j - H \sum_i S_i \ , \qquad (3)$$

where the parameter $-\alpha$ measures the relative strength of the next-nearest neighbor interaction. This choice of a model is also reasonable if one tries to fit real alloys, like the copper-gold system, in terms of a pairwise interaction model, Eq. (1) /5,6/. There is, however, at present no general agreement on whether this model (with parameters J,α smoothly depending on the relative composition c_B of the alloy, c_B being the thermal average $<c_i>_T$) is appropriate, or whether one needs a model with interactions between nearest neighbor pairs, triplets or quadruplets of atoms /7,8/. It might even be necessary to use explicitly the long-range interaction due to the conduction electrons of the metallic alloy /9/. In our opinion a considerable part of this uncertainty about an appropriate model for the ordering behavior of alloys is due to the fact that the properties of these models are not known with the precision needed to distinguish among them. As a step in this direction, the present paper presents a study of the model, Eq. (3), making use of the well-known Monte Carlo computer simulation method /10/. The phase diagram of this model system in the T-α plane at equal concentrations of A and B atoms (corresponding to H=0) has already been reported /11/. Some results at general composition have also been presented very briefly /12/ for the case α=0 with computations done in

the grand-canonical ensemble (H fixed as an independent variable). Here we present more extensive results of this latter work, supplementing it with computations done at other lattice sizes, computations in the canonical ensemble (c_B fixed as independent variable), and preliminary results for $\alpha \neq 0$. It turns out that even the nearest neighbor case ($\alpha = 0$, $H \neq 0$) is of great complexity: thanks to a large body of work /12-27/ the ground states of this model are quite well understood, but for nonzero temperature the approximation schemes available so far give greatly varying results /18-23/. As we shall see below, none of these schemes is completely satisfactory.

In Section 2 we give a description of the different computational procedures for the quantities of interest (order parameters, ordering energies, phase diagram). In Section 3 our results for $\alpha=0$ are presented and compared to other predictions /17-23/. Section 4 presents our results for $\alpha=-0.25$ and compares them to the cluster variatio (CV) predictions /4/, while Section 5 summarizes our conclusions.

2. The Monte Carlo Method

We consider a system of $N=4L^3$ spins on an fcc lattice with periodic boundary conditions. For the study of ordering phenomena, L has to be chosen such that the periodic boundary condition is compatible with the ordered structures expected. Fig. 1 shows some of the orderings which have been identified as ground-state orderings for our model /2,3/, translating them into the spin representation. While the AB structure of CuAuI-type as well as the A_3B structure of Cu_3Au-type (which both occur for $\alpha \geq 0$) fit the periodic boundary condition for any L, both the A_2B_2 structure and the A_3B structure of Al_3Ti type (which occur for $\alpha \leq 0$) fit the periodic boundary condition only for even L. For odd L this structure would necessarily require an interface ("domain wall"), which would disturb the results. Hence L=8 and L=16 (N=16384) were chosen to study these structures, and to make sure that finite size effects are already negligible (early work /24/ using L=5, i.e. N=500 and very short "observation times" could not study reliably the phase transitions, due to finite size- and finite time-effects). Finally, for the A_2B-structure, L has to be a multiple of 3 in order to avoid domain effects, as is obvious from Fig. 1e, and hence L=15 (i.e., N=13500) was chosen for studying that structure.

Similar considerations are possible for other structures which occur in the ground state /2,3/, such as the A_5B, A_4B and A_5B_3 structures. However, no attempt was made to study these structures at finite temperatures in the simulations: in the temperature regime of interest here ($k_BT/|J| \geq 0.3$) even the A_2B structure was never found to be stable, and we

expect a similar situation for these other more complicated structures, as will be discussed below.

In the case of $\alpha \neq 0$ the occurrence of long period superstructures (such as the CuAuII structure) is possible, and in other problems of Ising models with competing interactions such incommensurate structures have in fact been identified /25-27/. Since the periodic boundary condition is inconsistent with such structures for any finite L, the analysis of this case by Monte Carlo methods is rather delicate /25/. We do not consider this possibility here, since both in the theoretical models /25-27/ and in the experiments on the copper-gold system /28/ the regime of stability of the incommensurate phase in the phase diagram is very small.

The microscopic state of the system is specified by the configuration $\vec{X}, \vec{X}=\{S_1, S_2, \ldots, S_N\}$. When the system is at equilibrium, the probability of a configuration $\vec{X}$ is

$$P_{eq}(\vec{X}) = \frac{1}{Z} \exp[-\mathcal{H}(\vec{X})/k_B T], \quad Z = \sum_{\vec{X}} \exp[-\mathcal{H}(\vec{X})/k_B T] , \qquad (4)$$

where k_B is Boltzmann's constant and T the temperature of the system, $\mathcal{H}(\vec{X})$ being given by Eq. (3). Starting from an initial configuration $\vec{X}_o$ (the choice of which is discussed below), one lets the configuration of the system evolve according to the following algorithm /10/: using pseudorandom numbers one generates a random change of the configuration $\vec{X} \to \vec{X}'$. In the case of the grand-canonical ensemble { magnetic field in Eq. (3) is held fixed, concentration c_B is allowed to fluctuate} this transition $\vec{X} \to \vec{X}'$ is taken to be the flip $S_i \to -S_i$ of a randomly chosen spin.

In the case of the canonical ensemble, a nearest neighbor AB-pair is chosen at random and interchanged. This "Kawasaki dynamics" /29/ conserves the concentration c_B of the system. As is well known, both ensembles should yield results equivalent to each other in the thermodynamic limit $N\to\infty$. Since we work with finite N it is important to see that the results do not depend on the ensemble chosen, at least within reasonable error limits.

In both cases one computes the energy change $\delta U = \mathcal{H}(\vec{X}') - \mathcal{H}(\vec{X})$ resulting from the configurational change. The "transition probability" /10/ $W=\exp(-\delta U/k_BT)/[1+\exp(-\delta U/k_BT)]$ is then compared to a random number η, chosen uniformly from the interval [0,1]. If $W > \eta$ the transition is performed; otherwise the old configuration $\vec{X}$ is counted once more for the averaging, the attempted $\vec{X}'$ is rejected, and another transition is tried.

This algorithm is known /10/ to lead to the thermal equilibrium distribution, Eq. (4), in the limit where the number of states generated tends to infinity. In practice, one hopes to achieve accurate results when this number lies in the range from a few hundred to a few thousand Monte Carlo steps/site (MCS). To accomplish this aim, it is important to choose the initial states $\vec{X}_0$ appropriately. For runs using the grand-canonical ensemble, it is most convenient to use the fully ordered states (Fig. 1) as the initial condition. Although the ground-state is known to be highly degenerate for $\alpha=0$ /12-17/, it is known that at $T>0$ only the most symmetric structures contribute /30/. Thus for $\alpha=0$ only the structures of Fig. 1a,c,e were used, while for $\alpha=-0.25$ we used the structures of Fig. 1b,d. As

we shall see below, the transition from the ordered phases to the disordered one are of first order. Consequently, one has to pay attention to the occurrence of hysteresis: the limit of stability of the various ordered phases is not identical with the location of the first-order phase transition, but rather locates the regime where the lifetime of metastable states becomes short due to nucleation processes. Hence we also used states with a random or a ferromagnetic spin configuration as appropriate initial states for the disordered phase. As it is more difficult to create order out of disorder than vice versa, one finds even more pronounced metastability effects when one approaches the first-order transition from the disordered side. But by a careful analysis of the relaxation of the metastable states on both sides of the transition one can locate the phase boundary with reasonable accuracy /31/. This will become apparent from the detailed examples shown in Section 3.

For runs using the canonical ensemble, where the concentration c is kept at that of the initial state, the fully ordered configurations can be used as initial states only for the respective stoichiometric compositions. Non-stoichiometric initially ordered states could be produced by randomly changing the appropriate fraction of A-atoms into B-atoms (or vice versa) in such a fully ordered state. Most of our runs in the canonical ensemble were started from a random initial configuration.

We conclude this section by summarizing the definitions of the order parameters which we compute, paying attention to the appropriate translation from one ensemble to the other. Labelling the four sublattices of the unit cell of the fcc lattice as

indicated in Fig. 1, we introduce the sublattice magnetizations m_ν,

$$m_\nu = (1/N) \sum_{i\in\nu} \langle S_i \rangle , \qquad \nu=1,2,3,4 \tag{5}$$

where $\langle\ \rangle$ is computed by taking time averages over one or more Monte Carlo runs /10/. Then the order parameter components of the AB-structure (Fig. 1a) are expressed in terms of the m_ν as

$$\tilde{m}^{(1)}_{AB}=m_1+m_2-m_3-m_4,\ \tilde{m}^{(2)}_{AB}=m_1-m_2-m_3+m_4,\ \tilde{m}^{(3)}_{AB}=m_1-m_2+m_3-m_4 , \tag{6}$$

while the order parameter components of the A_3B-structure (Fig. 1c) are

$$\tilde{m}^{(1)}_{A_3B}=m_1+m_2+m_3-m_4,\ \tilde{m}^{(2)}_{A_3B}=m_1+m_2-m_3+m_4,\ \tilde{m}^{(3)}_{A_3B}=m_1-m_2+m_3+m_4,\ \tilde{m}^{(4)}_{A_3B}=-m_1+m_2+m_3+m_4 \tag{7}$$

Noting that $c_i=(1-S_i)/2$, the average magnetization m,

$$m=m_1+m_2+m_3+m_4 , \tag{8}$$

is related to the average concentration c_B of B atoms in the alloy by

$$c_B = (1-m)/2 . \tag{9}$$

The order parameter $\tilde{m}$ {Eqs. (6),(7)} is related to the standard long-range order parameter /1/ ψ by

$$\psi = (\tilde{m}-m)/(1-m) . \tag{10}$$

Short range-order in the grand-canonical ensemble is described

in terms of the correlation functions [$\vec{R}$ being the distance between sites i,j on the lattice]

$$g(\vec{R}) = \langle S_i S_{i+\vec{R}} \rangle - m^2 \tag{11}$$

This quantity is related to the standard Cowley short range order parameters $\alpha(\vec{R})$ /1,32/ by

$$\alpha(\vec{R}) = g(\vec{R})/(1-m^2) \tag{12}$$

In this paper, we only consider $\alpha_1 \equiv \alpha(\vec{R})$ for $\vec{R}$ a nearest-neighbor distance.

Finally we consider the energy U, which in the grand-canonical ensemble is defined as follows

$$U = \langle \mathcal{H} \rangle / N = U_{int} - mH \ ; \tag{13}$$

this quantity is related to the usual ordering energy /2/

$\Delta U = \sum_{i \neq j} \frac{1}{2}(2v_{ij}^{AB} - v_{ij}^{AA} - v_{ij}^{BB})[c_i(1-c_j) + c_j(1-c_i)]/N$ as

$$\Delta U = [U_{int} + J(0)] \ , \tag{14}$$

where $J(0) = \sum_{i \neq j} J_{ij}/N$. We note from Eqs. (11)-(14) that the ordering energy can be expressed in terms of the Cowley short range order parameters as

$$\Delta U = 4c_B(1-c_B)[J(0) - \sum_{i \neq j} J_{ij}\alpha(\vec{R})/N] \ . \tag{15}$$

In the case of only nearest neighbor interaction on the fcc lattice, Eq. (15) reduces to $\Delta U = 24 c_B (1-c_B) J (1-\alpha_1)$.

3. Results for the Nearest-Neighbor Interaction (α=0)

Figs. 2-4 show typical examples of "raw data" of the Monte Carlo computation. Most of the data were obtained in the grand-canonical (GC) ensemble, N=16384. It turned out that away from the transitions it was sufficient to average over 180 MCS/site, after omitting the initial 60 MCS/site of the simulation to get rid of the influence of the initial condition, while close to the transition averages were taken over 900 MCS/site. Runs using the canonical (C) ensemble were performed at the compositions c_B=0.225, 0.250, 0.265, 0.275, 0.30, 0.35, 0.40, 0.475 and 0.50, respectively. Identifying the corresponding field from the grand-canonical m vs. H-curve and Eq. (9), the energies and order parameters of the C and GC ensemble could be compared. Figs. 2-4 show that very good agreement between these two types of calculation was in fact obtained. In addition, data taken for different N agree with each other well.

From Figs. 2-4 we note that the magnetization varies linearly with the field in the disordered phase (and therefore so does the order parameter $\tilde{m}_{A_3B}$=m/2 in this range). In the regime with long-range order, however, the magnetization deviates from this simple linear law, and at the first-order transitions (occurring at one of the three critical fields H'_{c1}, H''_{c1} or H_{c2}, respectively) one can clearly identify the jump of the magnetization, $\Delta m = m_+ - m_-$, where $m_+(m_-) = \lim_{H \to H_c^+(H_c^-)} m(H)$. Since there is no one-phase equilibrium state with $m_- < m < m_+$, it is clear that states in this interval are two-phase mixtures, and hence one obtains the boundaries of the two-phase regions in the T-c phase diagram from using m_-, m_+ in Eq. (9). The critical fields are estimated by performing runs

with different initial conditions and searching for relaxation of metastable states, as mentioned in the previous section. Figs. 2,3 include a few examples of points where the A_3B ordering was found initially metastable while longer runs revealed a clear-cut relaxation towards the disordered phase.

Data as displayed in Figs. 2-4 have been taken at $k_BT/|J| =$ 0.3, 0.4, 0.6, 0.8, 1.0, 1.2, 1.4, 1.5, 1.6, 1.7, 1.75, 1.8, 1.85, 1.9, and 2.0, respectively, and thus the phase boundaries are constructed both in the $T-c_B$ representation (Fig. 5a) and in the T-H representation (Fig. 5b). We think that the relative accuracy of our estimates for the critical fields H'_{c1}, H''_{c1} (which merge at H_{c1} for $T \to 0$) is of the order of a few percent, i.e. the size of the circles in Fig. 5. The accuracy of the phase boundaries in the $T-c_B$ plane is better by about a factor of 2, because the "susceptibility" $\chi \equiv \partial m/(\partial H/|J|)$ is small. Note also (Fig. 2), that a small error in the location of the critical fields does not affect the magnitude of the jump of the magnetization very much, since (close to the respective critical fields) the m vs. H-curves are nearly parallel in the disordered phase and the A_3B phase. Therefore we think that meaningful estimates for the width of the two-phase regions have been obtained.

Fig. 6 shows the temperature variation of various quantities at fixed field. The estimated transition temperatures (taken from Fig. 5) are included. It is seen that pronounced superheating of the ordered phase (and supercooling of the disordered phase) occurs, when the transition temperature is low. This metastability is expected from the shape of the phase boundaries in Fig. 5, of course, since varying the temperature at either fixed

field or fixed composition one cuts the phase boundary typically at rather small angles. This is also the reason why in this case the computations in the canonical ensemble are convenient for locating the transition only for compositions near stoichiometry. Due to these hysteresis phenomena, no attempt was made to estimate the width of the two-phase region from the runs in the canonical ensemble. But apart from this latter ambiguity, both calculations give the same phase boundary, as is seen in Fig. 7 where we compare our results to the phase diagram predicted by the cluster variation (CV) method /20,22/. It is seen that the CV method overestimates the transition temperatures in the stoichiometric cases only by a few percent, while it is very inaccurate for intermediate compositions. In addition, it seems to underestimate somewhat the widths of the two-phase regions. An interesting feature, however, which is correctly predicted by the CV method is that the maximum transition temperature of the A_3B phase does <u>not</u> occur at the stoichiometric composition $c_B=1/4$ but rather for $c_B \cong 0.265$. It should also be noted, that simpler approximations (like the Bragg-Williams approximation, Bethe- and quasichemical approximations /18,19,21/) fail even more dramatically than the CV method, as they predict not only a wrong topology of the phase diagram, but cannot even locate the transition temperatures in the stoichiometric cases with reasonable accuracy (see /12/). On the other hand, the method of Wu and Tahir-Kheli /6/ (which refers to a model including 2^{nd} and 3^{rd} nearest neighbor interaction) predicts all transitions to the disordered phase to be of second order; even poorer are the real-space renormalization results /23/ which fail to yield the ordering of the AB phase, and predict the transition of the A_3B phase to be of second order. As a result, no analytic method

is presently capable to predict a satisfactory phase diagram for this model, and an extension of the methods of Refs. 6, 22 and 23 seems to be called for.

While the CV method predicts a triple point at nonzero temperature T_t, below which one can observe transitions from the A_3B structure to the AB structure, we have tentatively extrapolated our results (Fig. 5) such that T_t=0. Some justification of this extrapolation is found when one considers the ground-state energy as function of composition (Fig. 8a) or field (Fig. 8b). It turns out that the variation with composition is much more complicated to understand than the behavior as function of the field. While for $\alpha \to 0^+$ the ground state is a two phase mixture of pure A and A_3B phases for $0 < c_B < \frac{1}{4}$, and of A_3B,AB phases for $\frac{1}{4} < c_B < \frac{1}{2}$, several other phases occur for $\alpha \to 0^-$ /2,3/. One first has a transition to a (nonstoichiometric) A_5B phase; but the location of this transition is uncertain. At c_B=1/6 one starts to have a three-phase mixture, containing the A_5B,A_4B and A_3B phases. In view of this situation, it is interesting to note that the outer boundary of the two-phase region between the disordered and the A_3B phase seems to extrapolate towards c_B=1/6(Fig. 5). For $\frac{1}{4} < c_B < \frac{1}{3}$ a two-phase mixture between A_3B and A_2B is predicted, while for c_B>1/3 a two-phase mixture between A_2B and A_5B_3 should occur which has a transition (at a so far unknown concentration) to a pure non-stoichiometric A_5B_3 phase.

Unfortunately, we have not been able to establish the connection between these ground-state phases and the behavior seen at nonzero temperature. In particular, starting the

system in the A_2B structure revealed that this structure was not stable (and not even metastable) down to $k_BT/|J| \approx 0.3$, and we expect that it will not be stable at any nonzero temperature.

The reason for the different instability of the various ordered phases is seen more clearly in Fig. 8b, which shows that the AB and A_3B structures are ground state arrangements for extended intervals of the field, while A_5B_3 and A_2B are groundstates only just at the critical field $H_{c1}/|J|=4$, and A_4B as well as A_5B are groundstates only right at the critical field $H_{c2}/|J|=12$. On the other hand, just at the critical field the system is so degenerate that it has a finite entropy. Using boundary conditions which do not favor a particular ordering leads to a disordered system /12,17/. This fact can be most easily seen from the following simple argument /12/. Consider two neighboring cells of the A_3B structure (Fig. 9a), and focus attention upon the spin in the center of the plane joining the cells. Four of its bonds to nearest neighbors are energetically favorable (drawn dash-dotted) while the other eight are unfavorable (drawn broken). Therefore at the critical field H_{c1} this spin can be overturned with no energy cost. Since there are no bonds between spins on the same sublattice, we have two degenerate states for <u>every</u> spin on this sublattice if we keep the spin configuration of the three other sublattices fixed. As a result we would have one sublattice of down spins, two sublattices of up spins and one sublattice disordered, i.e. a ground-state entropy of $S_o=(\ell n2)/4$ and magnetization $m_o=1/4$ ($c_B=3/8$) at the critical field. Of course, this picture of perfect order on three sublattices and perfect disorder on the fourth is too simple (yielding however a lower bound on S_o). What we rather expect to

happen is a disordering of all sublattices, where short-range correlations are created. Consider as an example a group of eight cells (Fig. 9b) where four such loose spins, which are nearest neighbors on their sublattice, have been turned around: now it is a spin of the other sublattice in the "antiferromagnetic" plane which is loose and can be turned around. A similar degeneracy exists for spins in the "ferromagnetic" planes of the A_3B structure (Fig. 9c). It is not clear to what extent the above simple estimates of S_o and m_o are modified by this more complicated disorder. The Monte-Carlo results at $T\neq 0$ for $H=H_{c1}$ are extremely close to $m=1/4$, however; thus the extrapolation of the phase boundaries between the disordered phase and the two-phase regime ending at the point $T=0$, $c_B=3/8$ may have some significance. We did not attempt to extrapolate the phase boundaries between the ordered phases and the two-phase regimes, however. Studying the low-temperature behavior by Monte Carlo methods is rather delicate, as the convergence may be strongly slowed down for $T \to 0$, and metastable states can hardly be distinguished from stable ones.

Fig. 10 presents an example for the results on order parameters obtained in the present study. While the Cowley short range order parameter $-\alpha_1$ increases monotonically with concentration c_B up to $c_B=1/2$ at high temperatures, it develops a minimum at lower temperatures around $c_B=3/8$. This behavior also reflects the fact that in the vicinity of this concentration there is much less ordering tendency, as noted above from ground-state considerations. At lower temperatures and stoichiometric compositions α_1 soon reaches its saturation values (A_3B structure: $\alpha_1=-1/3$, AB struc-

ture: α_1=-1/3), while it varies linearly with c_B in the two-phase regions. At the stoichiometric compositions, the temperature variation of the order parameters is found to be neither very sensitive to the model nor the approximation, as Fig. 10 shows, and even experimental data for the Au_3Cu-system /33/ are in rough agreement with the calculation. However, from the phase diagram of the present model (Fig. 5) it is already clear that it cannot represent the experimental Au_3Cu system. Thus we suggest that one can check both the accuracy of a model as well as the accuracy of approximations when one studies off-stoichiometric compositions.

Fig. 11 shows the concentration dependence of ordering energy and long range order parameter. It is seen that the ordering energy changes very little throughout the ordered regime and even above the maximum transition temperature it is close to the variation in the ground state. This is again a reflection of the fact that both energy differences and entropy differences between the various ordered phases are very small, and hence the entropy of the phases needs to be calculated very accurately, if one wants to make reliable predictions about the ordering behavior of this model system. This is probably the reason why many approximate methods give such unreliable results.

At low temperatures, the long range order parameter of the A_3B structure has its maximum at the stoichiometric composition, but at higher temperatures it occurs at $c_B \cong 0.26$ rather than at c_B=0.25, consistent with our finding that the maximum transition temperature of this phase occurs at $c_B \cong 0.265$ (Fig. 7).

We find that the transition to the disordered phase occurs typically when the long range order parameter has decreased to roughly 0.6 to 0.7. This may perhaps be understood as coming from "frustration". The system can not maintain itself in a state of long range order - there are too many opportunities for spins to flip. This results in a complete break-down of the ordered state and thus in a first order transition.

4. Results for a Next-Nearest Neighbor Alloy (α=-0.25)

Recently Sanchez and de Fontaine /4/ applied the CV method to obtain the temperature-composition phase diagram of the alloy at α=-0.25. This was our motivation to perform canonical ensemble Monte Carlo calculations at c_B=0.25 and c_B=0.50. We find the transitions to be of first order, in agreement with the CV prediction, and estimate $k_B T_c/|J| = 1.116 \pm 0.002$ (c_B=0.25), while the CV result is $k_B T_c/|J| = 1.17$ /4/. A similar deviation of only a few percent occurs for c_B=0.5 where we get $k_B T_c/|J| = 1.431 \pm 0.004$, while the CV result is /4/ $k_B T_c/|J| = 1.50$. Thus again the CV method is quite reliable for the stoichiometric compositions. Preliminary results at c_B=0.33 indicate that the CV method is less reliable at non-stoichiometric compositions also in this case.

Since a fairly complicated phase diagram has been predicted (Fig. 12), a more complete investigation of this system by Monte Carlo methods would be desirable, but this is beyond the scope of the present investigation.

5. Summary

We have given a detailed description of the Monte Carlo method for the study of alloy phase diagrams, order parameters etc., and described results for the face-centered cubic lattice with nearest neighbor interaction in detail. We have found that the phase diagram obtained from approximate analytic methods are generally not very reliable. Only the cluster variation method with tetrahedral clusters has yielded both transition temperatures and order parameters reliably (i.e., within an error of at most a few percent), for stoichiometric compositions. Other approximate methods used so far are quite inaccurate even then. The present results are therefore a challenge to develop better theoretical methods for the calculations of phase diagram of these "frustrated-type" systems. Further work on the cluster variation method with higher order clusters also seems very desirable. Needless to say we have only considered a very simple model, which is not expected to represent faithfully any real alloy system - but more complicated realistic interactions are not likely to make the currently available approximation methods any more reliable. The methods are insufficient in our case because the treatment of configurational entropy of the alloy is too crude, and this fact will likely also be true in the more complicated cases. Computer simulation methods do appear to yield numerically accurate information on both short and long range order parameters and the phase diagram, but they are expensive to use because of the large amounts of computer time required; and the computations have to be repeated for each set

of parameters. Nevertheless, in future work we hope to apply the same methods to more complicated models which are closer to real systems. As a first step in this direction we have given a few results for an alloy with a next-nearest neighbor interaction.

Some conclusions which emerge from this study may stimulate more experimental work on ordering alloys. We have found that the behavior of stoichiometric alloys is rather insensitive to the parameters of the model, and to the accuracy of the approximations used. On the other hand, observing concentration dependences of long- and short range order parameters (Figs. 10,12) would be much more sensitive tool for checking whether a model faithfully represents a real system.

There have also been developed recently some rigorous methods for describing the phase diagram of complex alloy systems at low temperatures.[34,30] Unfortunately these methods are restricted at the moment to very low temperatures and require that the degeneracy of the ground state be finite. As we have noted this is not the case at the "interesting" values of the field and of the composition at least for the model studied here. Fortunately this restriction may soon be removed.[35]

Acknowledgements

We wish to thank D. Mukamel and J. Slawny for very useful discussions. J.L.L. would also like to thank Prof. N. Kuiper for his hospitality at IHES where part of this work was done. We thank D. de Fontaine and R. Kikuchi for their comments on the manuscript.

References

/1/ For a review and general references, see D. de Fontaine, in Solid State Physics, edited by H. Ehrenreich, F. Seitz and D. Turnbull (Academic, New York, 1979), Vol. 34, p. 73.

/2/ M.J. Richards and J.W. Cahn, Acta Met. 19, 1263 (1971).

/3/ S.M. Allen and J.W. Cahn, Acta Met. 20, 423 (1972); Scripta Met. 7, 1261 (1973).

/4/ J.M. Sanchez and D. de Fontaine, Phys. Rev. B21, 216 (1980).

/5/ P.C. Clapp and S.C. Moss, Phys. Rev. 171, 754 (1968); 764 (1968); 172, 418 (1968).

/6/ D.-H. Wu and R.A. Tahir-Kheli, J. Phys. Soc. Japan 31, 641 (1971).

/7/ C.M. van Baal, physica 64, 571 (1973).

/8/ D. de Fontaine and R. Kikuchi, NBS Publication SP-496, 999 (1978).

/9/ R.C. Kittler and L.M. Falicov, Phys. Rev. B18, 2506 (1978); B19, 291 (1979).

/10/ For a recent introduction to this method see K. Binder (ed.), Monte Carlo Methods in Statistical Physics (Springer, Berlin-Heidelberg-New York, 1979).

/11/ M.K. Phani, J.L. Lebowitz, M.H. Kalos and C.C. Tsai, Phys. Rev. Lett. 42, 577 (1979); M.K. Phani, J.L. Lebowitz and M.H. Kalos, Phys. Rev. B (1980).

/12/ K. Binder, Phys. Rev. Lett. (1980).

/13/ P.W. Anderson, Phys. Rev. 79, 705 (1950).

/14/ J.M. Luttinger, Phys. Rev. 81, 1015 (1951).

/15/ A. Danielian, Phys. Rev. Lett. 6, 670 (1961); Phys. Rev. 133A, 1344 (1964).

/16/ S. Alexander and P- Pincus, J. Phys. A13, 263 (1980).

/17/ O.J. Heilmann, J. Phys. A13, 1803 (1980).

/18/ W. Shockley, J. Chem. Phys. 6, 130 (1938).

/19/ Y.Y. Li, J. Chem. Phys. 17, 447 (1949).

/20/ N.S. Golosov, L.E. Popov, and L.Y. Pudan, J. Chem. Solids 34, 1149 (1973); 34, 1159 (1973).

/21/ R. Kikuchi and H. Sato, Acta Met. 22, 1099 (1974).

/22/ R. Kikuchi, J. Chem. Phys. 60, 1071 (1974).

/23/ G.D. Mahan and F.H. Claro, Phys. Rev. B16, 1168 (1977).

/24/ L.D. Fosdick, Phys. Rev. 116, 565 (1959).

/25/ W. Selke and M.E. Fisher, Phys. Rev. B20, 257 (1979); E.B. Rasmussen and S.J. Knak-Jensen, preprint.

/26/ R. Kretschmer and K. Binder, Z. Physik B34, 375 (1979)

/27/ Y. Saito, preprint.

/28/ M. Hansen, Constitution of Binary Alloys, McGraw Hill Book Co., New York (1958).

/29/ K. Kawasaki, in Phase Transitions and Critical Phenomena, ed. by C. Domb and M.S. Green (Academic, New York 1972), Vol. 2, p.443.

/30/ J. Slawny, J. Stat. Phys. 20, 711 (1979).

/31/ For a more detailed discussion of this problem, see D.P. Landau and K. Binder, Phys. Rev. B17, 2328 (1978).

/32/ J.M. Cowley, Phys. Rev. 77, 669 (1950).

/33/ D.T. Keating and B.E. Warren, J. Appl. Phys. 22, 286 (1951); see also S.C. Moss, J. Appl. Phys. 35, 3547 (1964).

/34/ G.A. Progov and Y. Sinai, Teor. Math. Fiz. 25, 358 (1975); 26, 61 (1976). W. Holsztynski and J. Slawny, Comm. Math. Phys. 61, 177 (1978).

/35/ J. Slawny, private communication.

Figure Captions

Fig. 1: a) One cube of the fcc lattice shown for the AB structure of CuAuI-type, A-atoms being represented as "spin up", B-atoms as "spin down"; b) two cubes, A_2B_2 structure; c) one cube, A_3B structure of Cu_3Au-type; d) two cubes, A_3B structure of Al_3Ti-type; e) six cubes, A_2B structure of Ni_2V-type. Numbers in case a) indicate the sublattice labelling.

Fig. 2: Internal energy (upper part), order parameters (middle part) and magnetization (lower part) of the nearest-neighbor Ising antiferromagnet plotted vs. field at $k_BT/|J|=1.5$. Both data from canonical (C) and grand canonical (GC) simulations are included. Points with arrows denote states with unstable ordering relaxing towards the disordered phase. The estimates for the three critical fields H'_{c1},H''_{c1} and H_{c2} are also indicated.

Fig. 3: Internal energy (upper part), order parameters (middle part) and magnetization (lower part) of the nearest-neighbor Ising antiferromagnet plotted vs. field at $k_BT/|J|=1.7$.

Fig. 4: Internal energy (upper part), order parameter $\tilde{m}_{A_3B}$ (middle part) and magnetization (lower part) of the nearest-neighbor Ising antiferromagnet plotted vs. field at $k_BT/|J|=2.0$.

Fig. 5: Phase diagram of the nearest-neighbor face-centered cubic lattice in the temperature-composition plane (upper part) and in the temperature-field plane. Ordered structures are indicated. All transitions are found to be of first order. Open circles represent the estimates for the critical fields H'_{c1},H''_{c1} and H_{c2} mentioned in the text.

Fig. 6: Temperature variation of the magnetization (upper part), order parameter $\tilde{m}_{A_3B}$ (middle part) and internal energy (lower part) for various values of the field. Broken curves indicate metastable states.

Fig. 7: Temperature-composition phase diagram of the fcc binary alloy with nearest-neighbor interaction. Full curves are the prediction of the cluster variation method in the tetrahedron approximation /22/. Note that in the pairwise interaction model all phase diagrams are symmetric around $c_B=1/2$.

Fig. 8: Variation of the ordering energy at T=0 with composition (a) /2,3/ or field (b). The various ordered structures (or mixtures of them) are indicated.

Fig. 9: Configurations of neighboring cells in the A_3B structure where spins become "loose" at the critical field H_{c1}. For explanations cf. text.

Fig. 10: Variation of the Cowley short range order (SRO) parameter α_1 with composition (upperpart) and plot of α_1 and long range order parameter (LRO) ψ vs. temperature at $c_B=1/4$ (lower part). Full curves are the MC results, broken curves the CV method (Ref. 20), dash-dotted curve the Kittler-Falicov thecry (Ref. 9), open circles are experimental data for $AuCu_3$ (Ref. 33).

Fig. 11: a) Ordering energy of the fcc nearest neighbor alloy plotted vs. composition at two temperatures. b) Long range order parameter plotted vs. composition at three temperatures. Dots denote Monte Carlo results obtained from GC calculations. Broken straight lines indicate the two-phase regime.

Fig. 12: Phase diagram of the fcc next nearest neighbor alloy (α=-0.25) according to the cluster variation method /4/. Points denote present Monte Carlo results for the transition temperatures at c_B=1/4 and c_B=1/2.

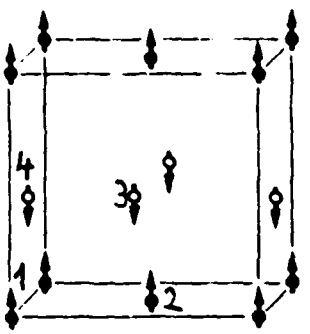

a) AB (Cu Au I)

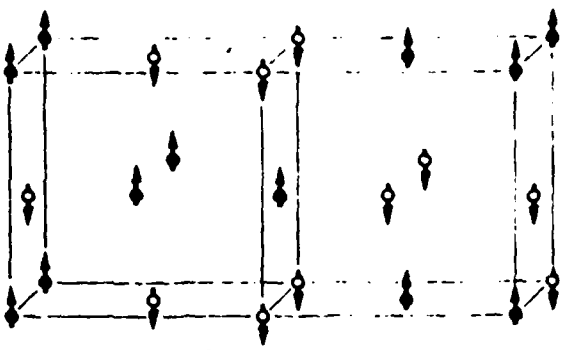

b) A_2B_2

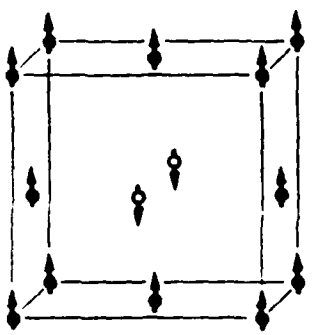

c) A_3B (Cu_3Au)

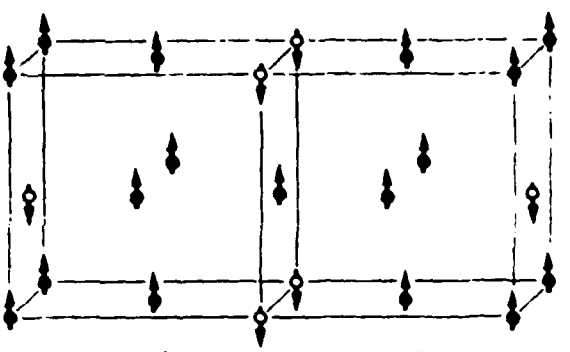

d) A_3B (Al_3Ti)

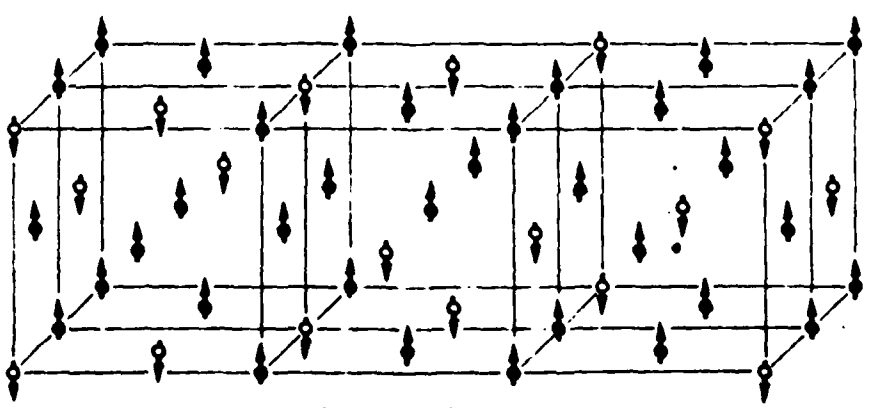

e) A_2B (Ni_2V)

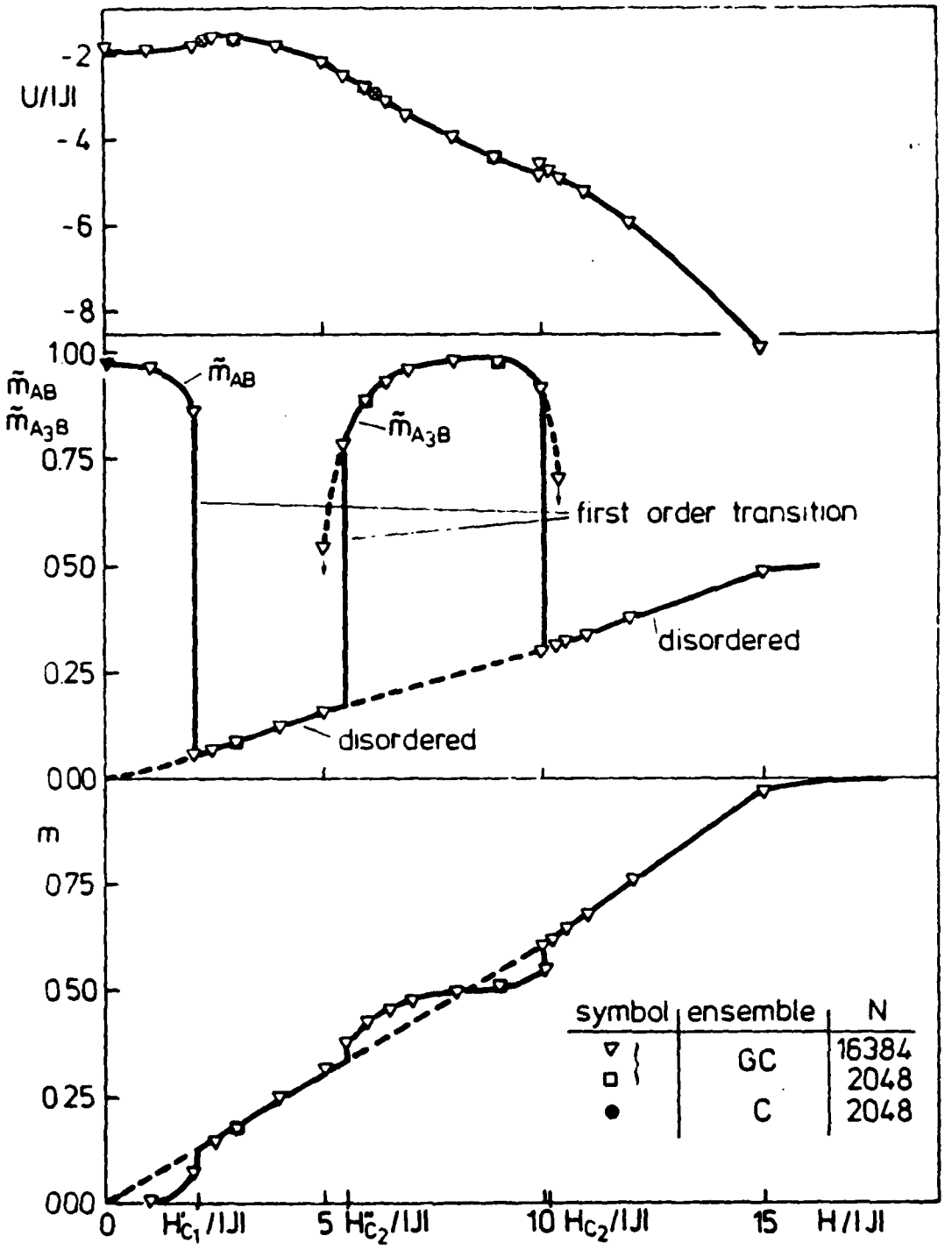
-2
U/|J|
-4
-6
-8
1.00
$\tilde{m}_{AB}$
$\tilde{m}_{A_3B}$
0.75
0.50
0.25
0.00
$\tilde{m}_{AB}$
$\tilde{m}_{A_3B}$
first order transition
disordered
disordered
m
0.75
0.50
0.25
0.00
symbol
ensemble
N
GC
16384
2048
C
2048
0
$H_{c_1}/|J|$
5 $H_{c_2}/|J|$
10 $H_{c_2}/|J|$
15
H/|J|

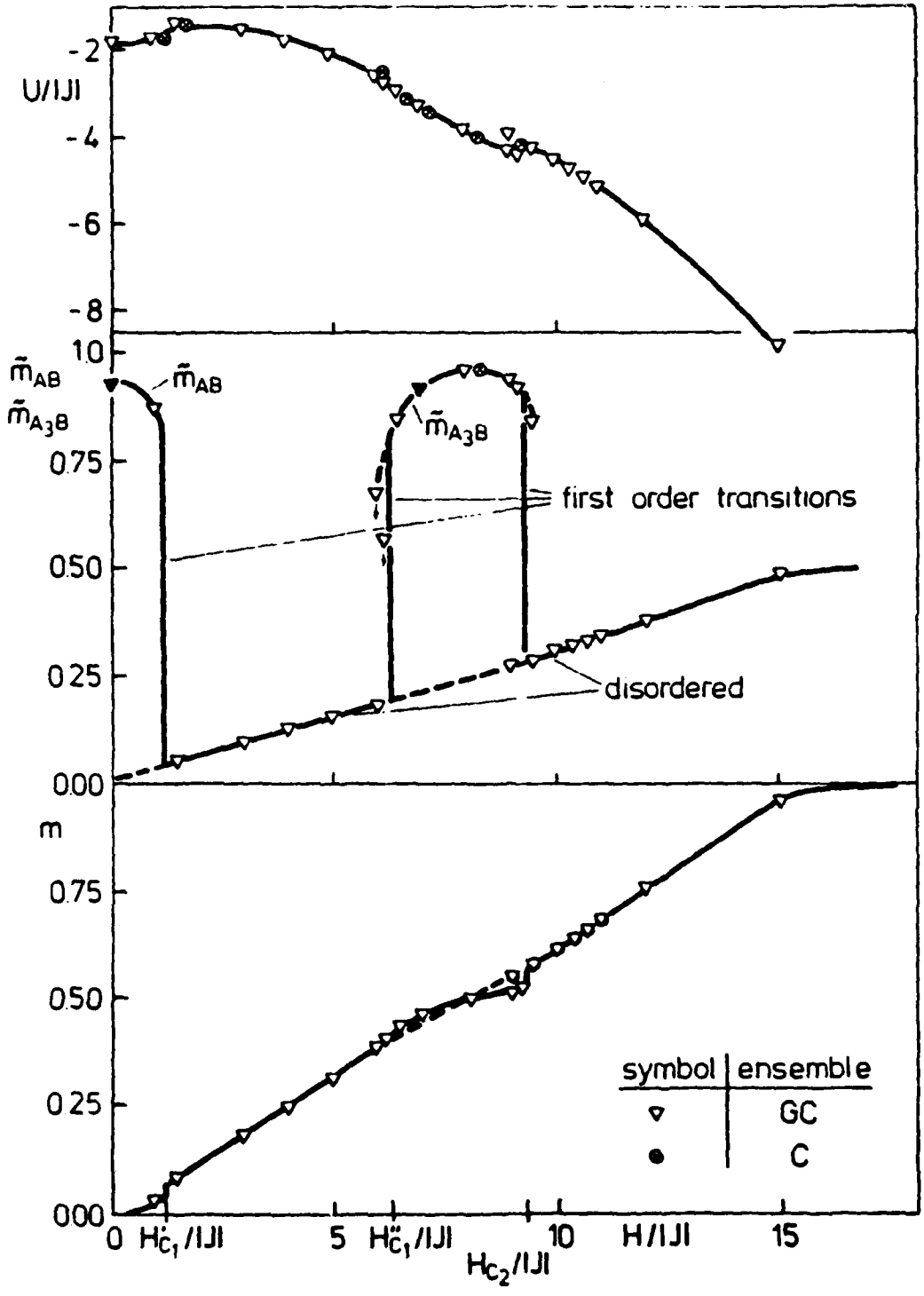
-2
U/|J|
-4
-6
-8
1.0
$\tilde{m}_{AB}$
$\tilde{m}_{A_3B}$
0.75
0.50
0.25
0.00
$\tilde{m}_{AB}$
$\tilde{m}_{A_3B}$
first order transitions
disordered
m
0.75
0.50
0.25
0.00
symbol | ensemble
GC
C
0
$H_{c_1}'/|J|$
5
$H_{c_1}''/|J|$
10
$H/|J|$
15
$H_{c_2}/|J|$

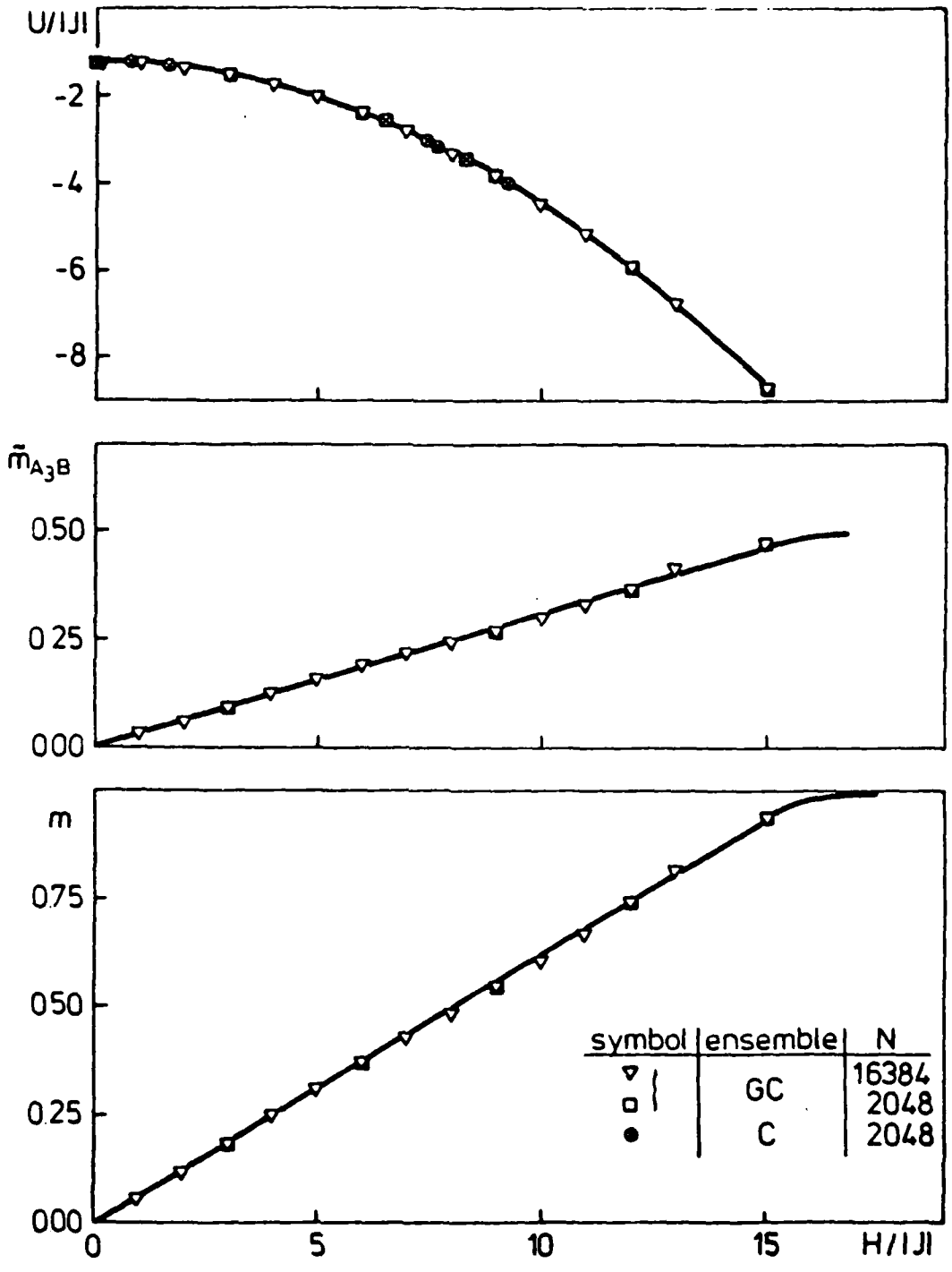
U/|J|
-2
-4
-6
-8
$\tilde{m}_{A_3B}$
0.50
0.25
0.00
m
0.75
0.50
0.25
0.00
0
5
10
15
H/|J|
symbol
ensemble
N
GC
16384
2048
C
2048

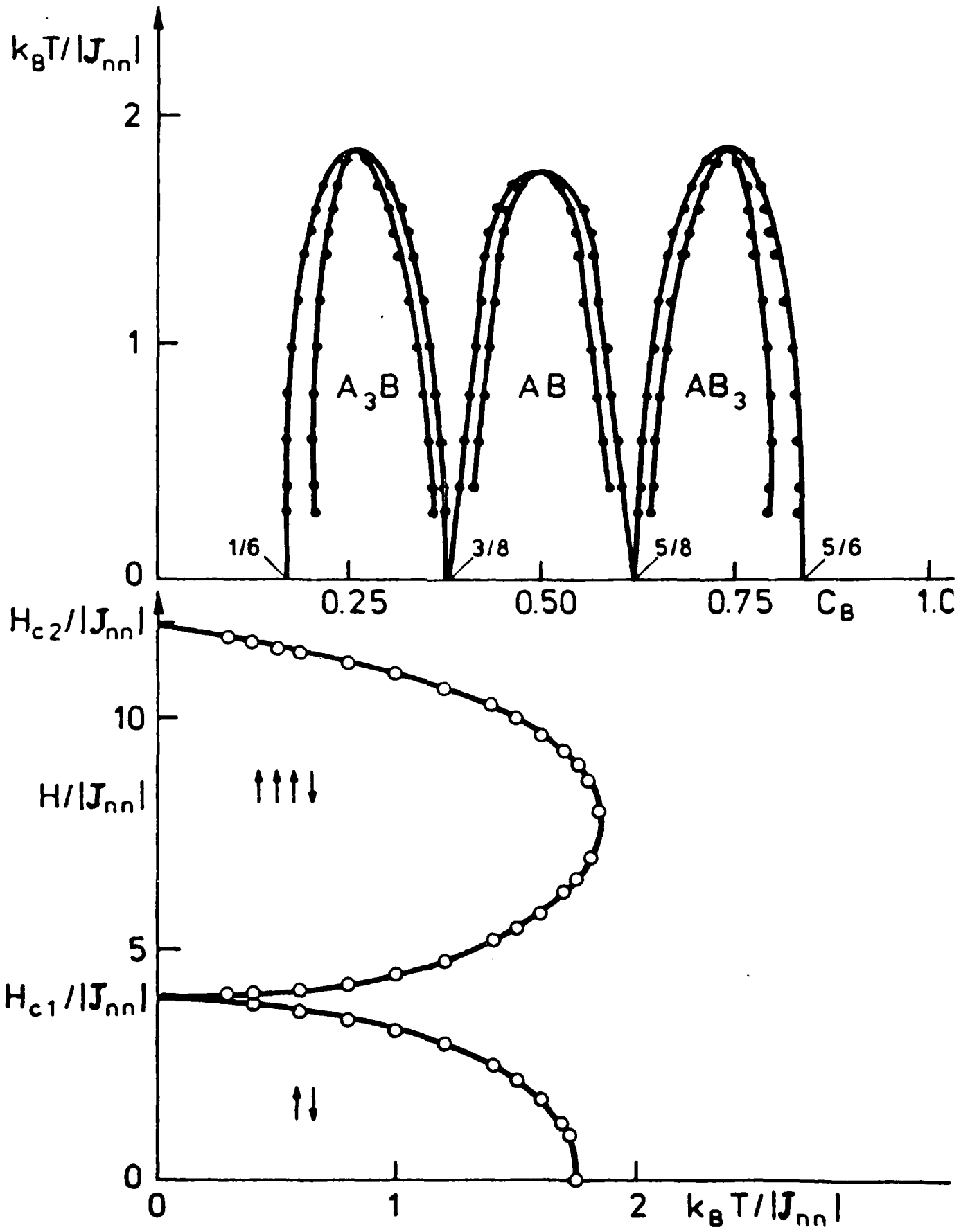
$k_BT/|J_{nn}|$
2
1
0
A_3B
AB
AB_3
1/6
3/8
5/8
5/6
0.25
0.50
0.75
C_B
1.0
$H_{c2}/|J_{nn}|$
10
$H/|J_{nn}|$
5
$H_{c1}/|J_{nn}|$
0
0
1
2
$k_BT/|J_{nn}|$

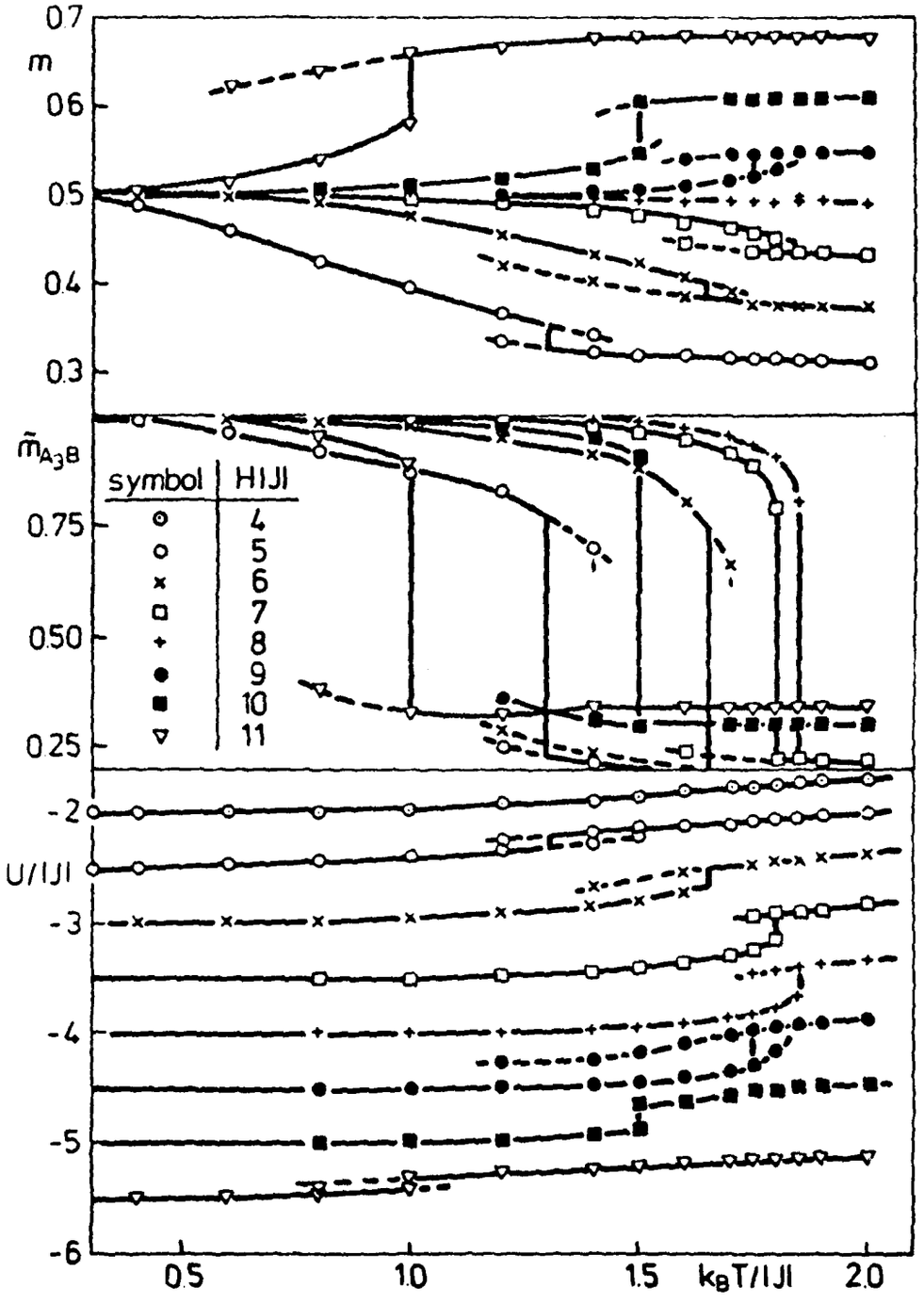
0.7
m
0.6
0.5
0.4
0.3
$\tilde{m}_{A_3B}$
symbol | H|J|
4
5
6
7
8
9
10
11
0.75
0.50
0.25
-2
U/|J|
-3
-4
-5
-6
0.5
1.0
1.5
$k_BT/|J|$
2.0

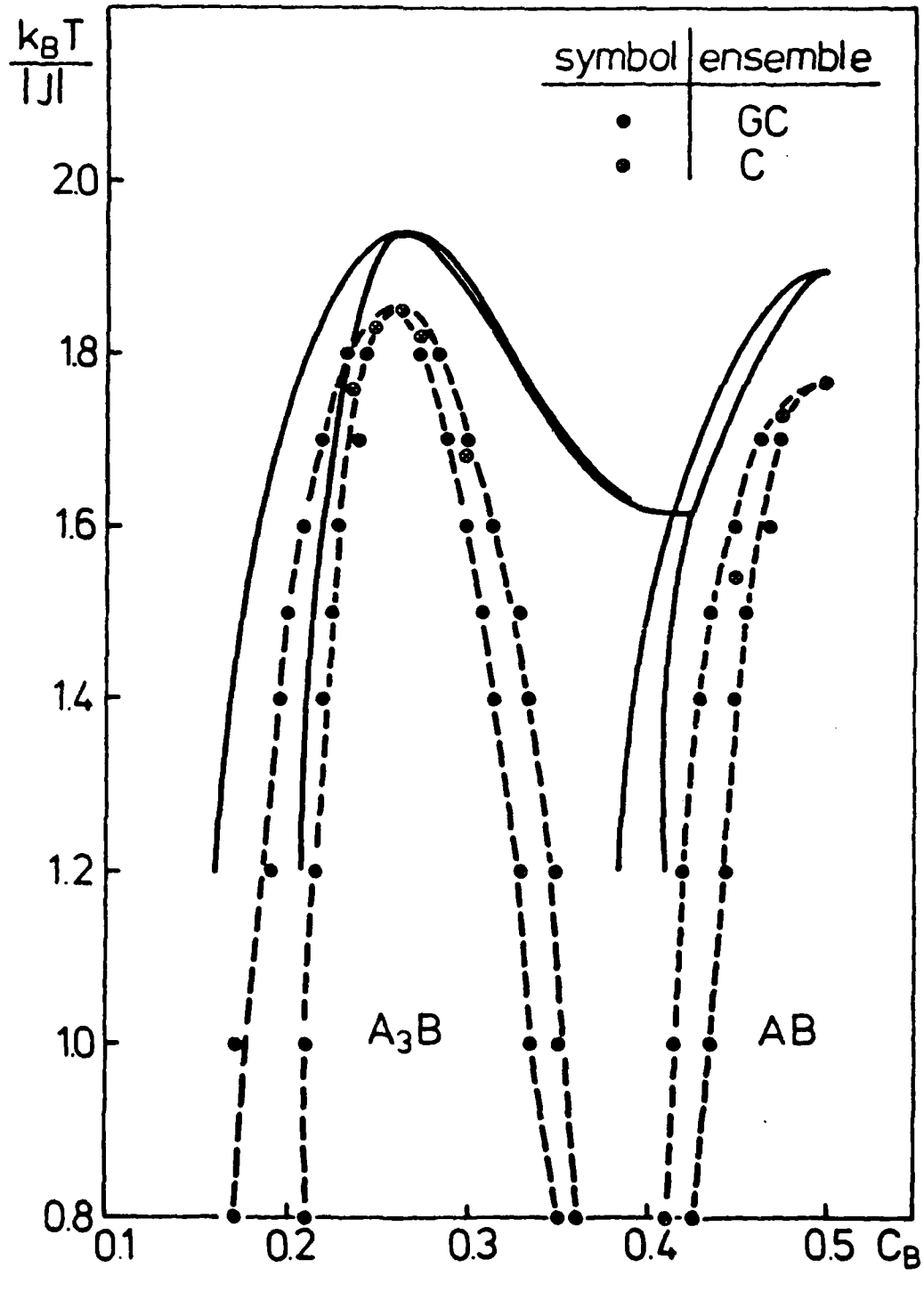
$\frac{k_B T}{|J|}$
symbol | ensemble
GC
C
2.0
1.8
1.6
1.4
1.2
1.0
0.8
0.1
0.2
0.3
0.4
0.5
C_B
A_3B
AB

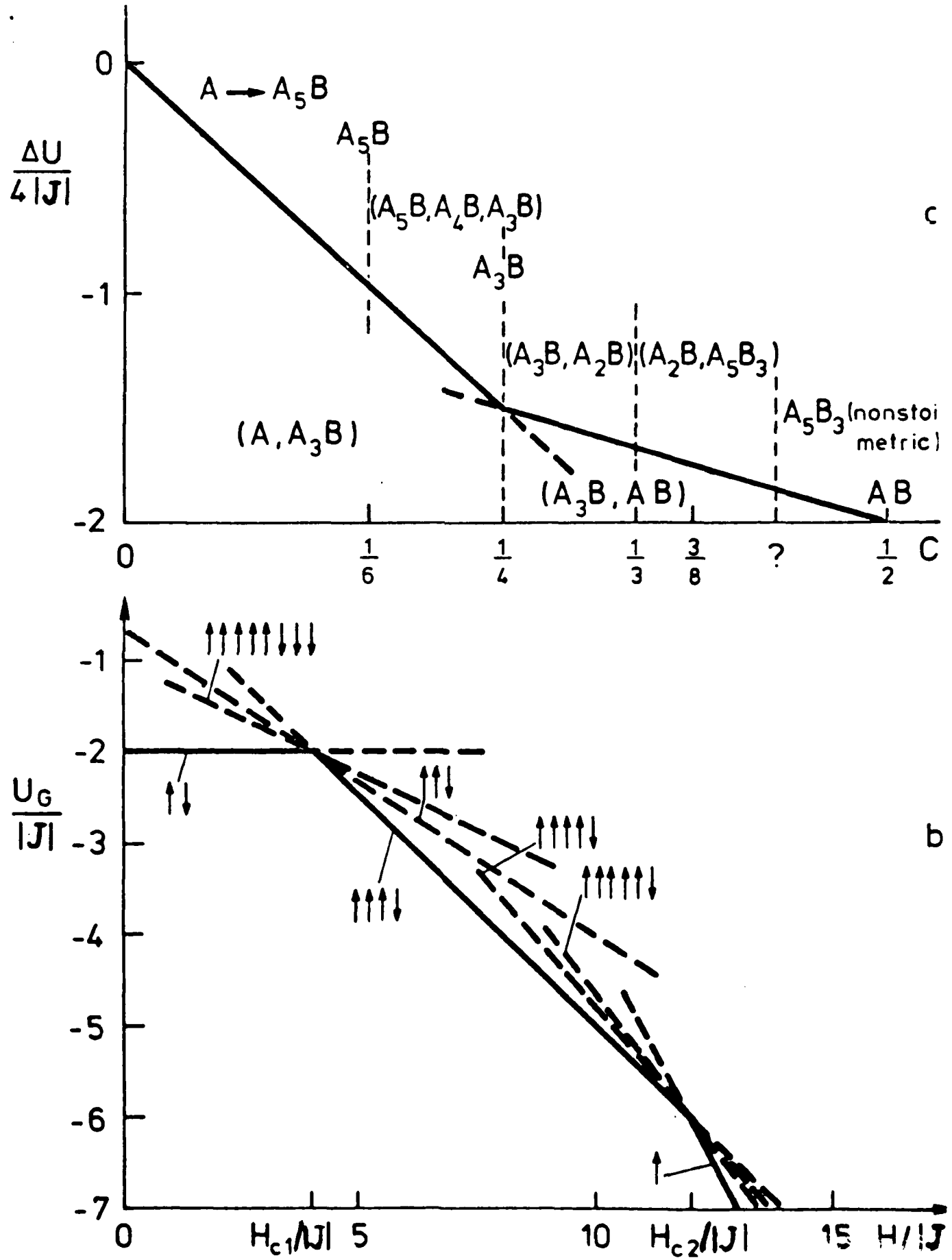
0
-1
-2
$\frac{\Delta U}{4|J|}$
A → A_5B
A_5B
(A_5B, A_4B, A_3B)
A_3B
(A_3B, A_2B)
(A_2B, A_5B_3)
A_5B_3 (nonstoi metric)
(A, A_3B)
(A_3B, AB)
AB
c
0
$\frac{1}{6}$
$\frac{1}{4}$
$\frac{1}{3}$
$\frac{3}{8}$
?
$\frac{1}{2}$
C

-1
-2
-3
-4
-5
-6
-7
$\frac{U_G}{|J|}$
b
0
$H_{c1}/|J|$
5
10
$H_{c2}/|J|$
15
$H/|J$

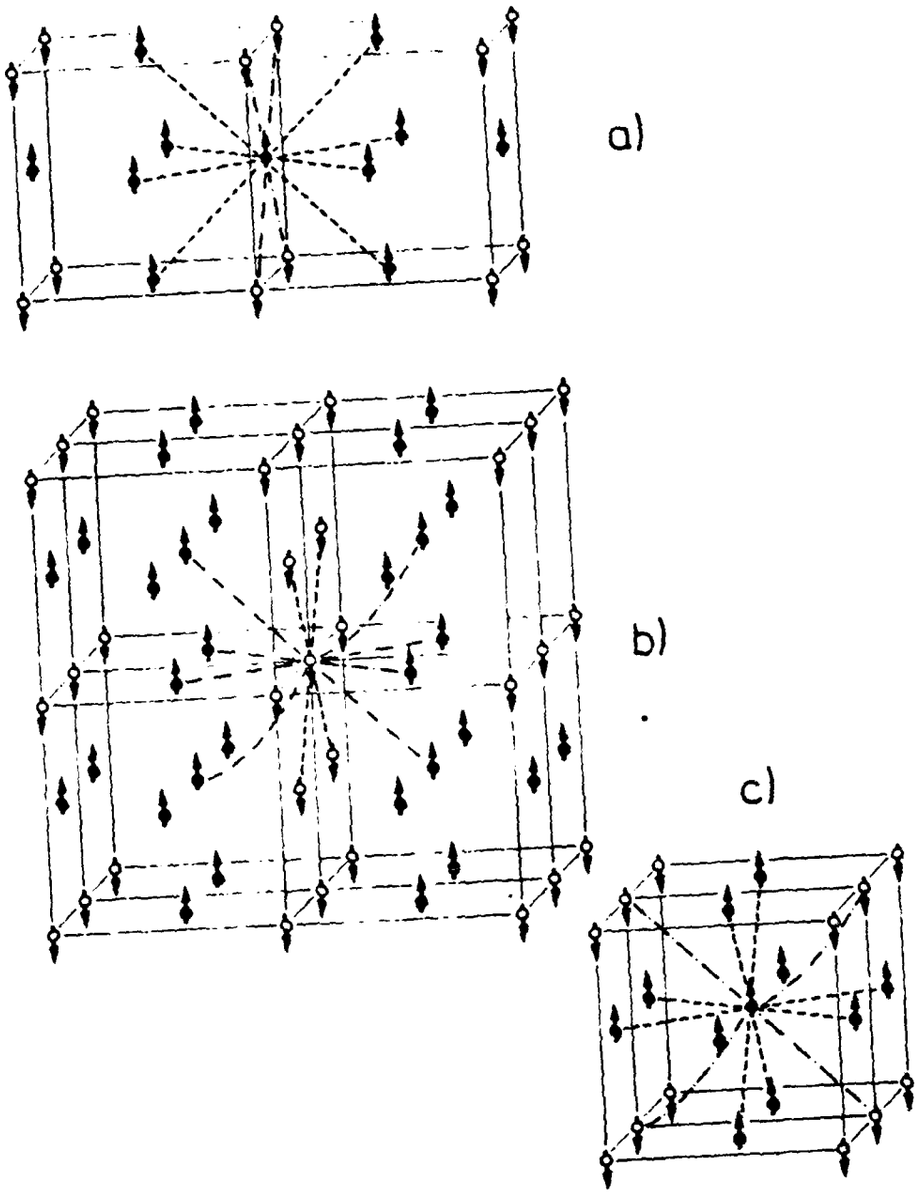
a)
b)
c)

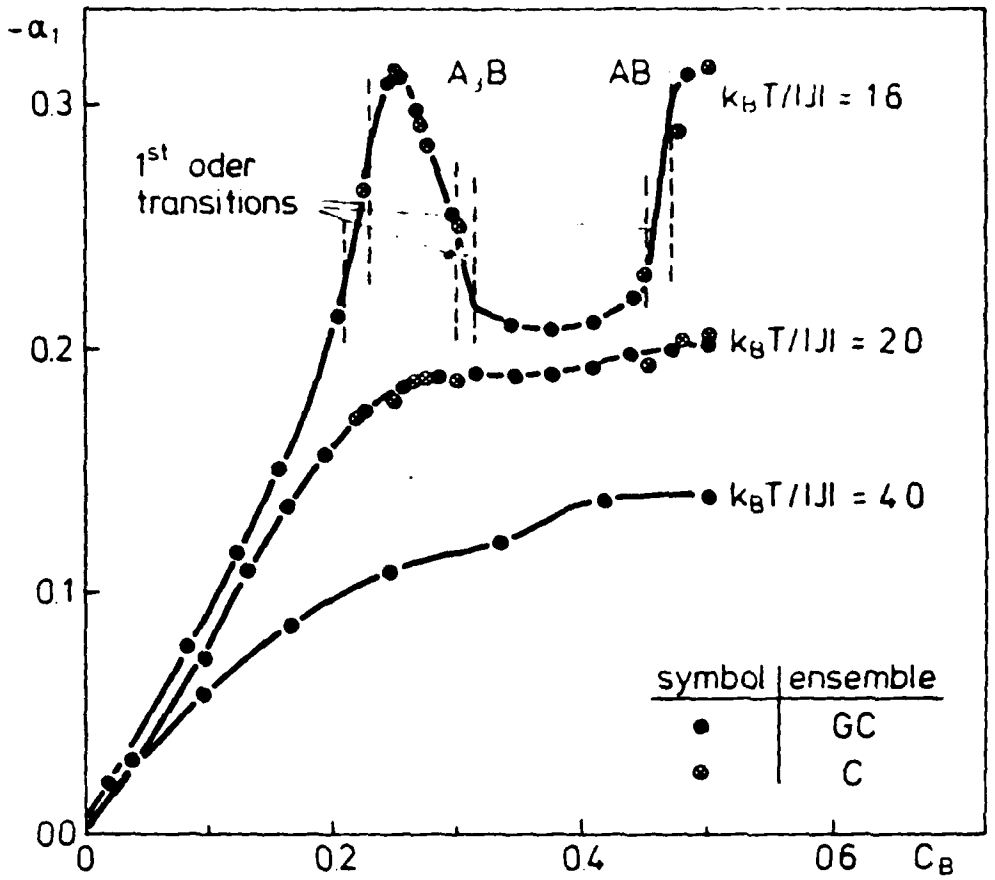
$-\alpha_1$
0.3
0.2
0.1
0.0
0
0.2
0.4
0.6
C_B
A_3B
AB
$k_BT/|J|$ = 1.6
$k_BT/|J|$ = 2.0
$k_BT/|J|$ = 4.0
1st oder transitions
symbol | ensemble
GC
C

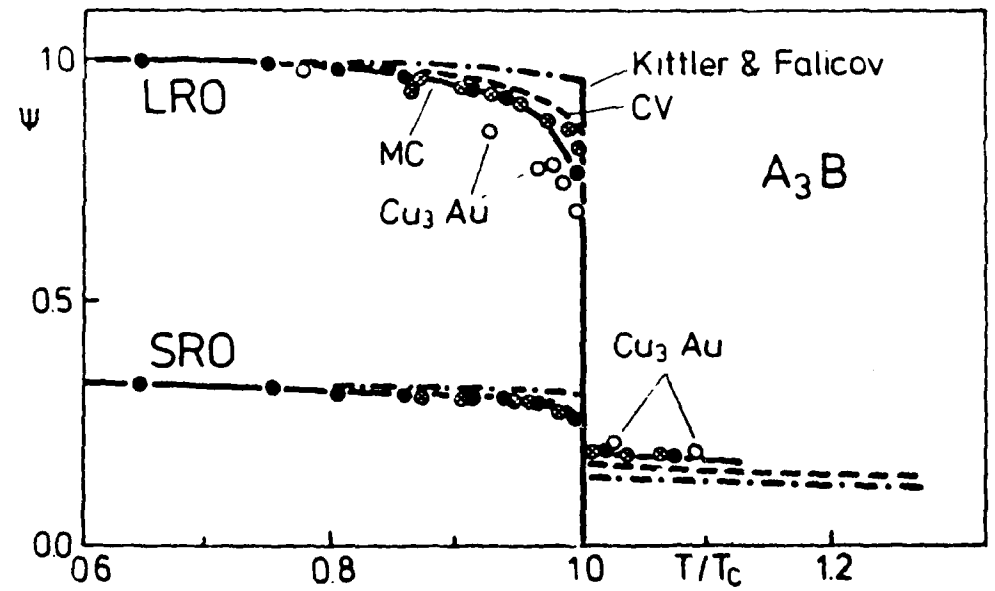
1.0
0.5
0.0
ψ
LRO
SRO
Kittler & Falicov
CV
MC
Cu_3Au
A_3B
Cu_3Au
0.6
0.8
1.0
T/T_C
1.2

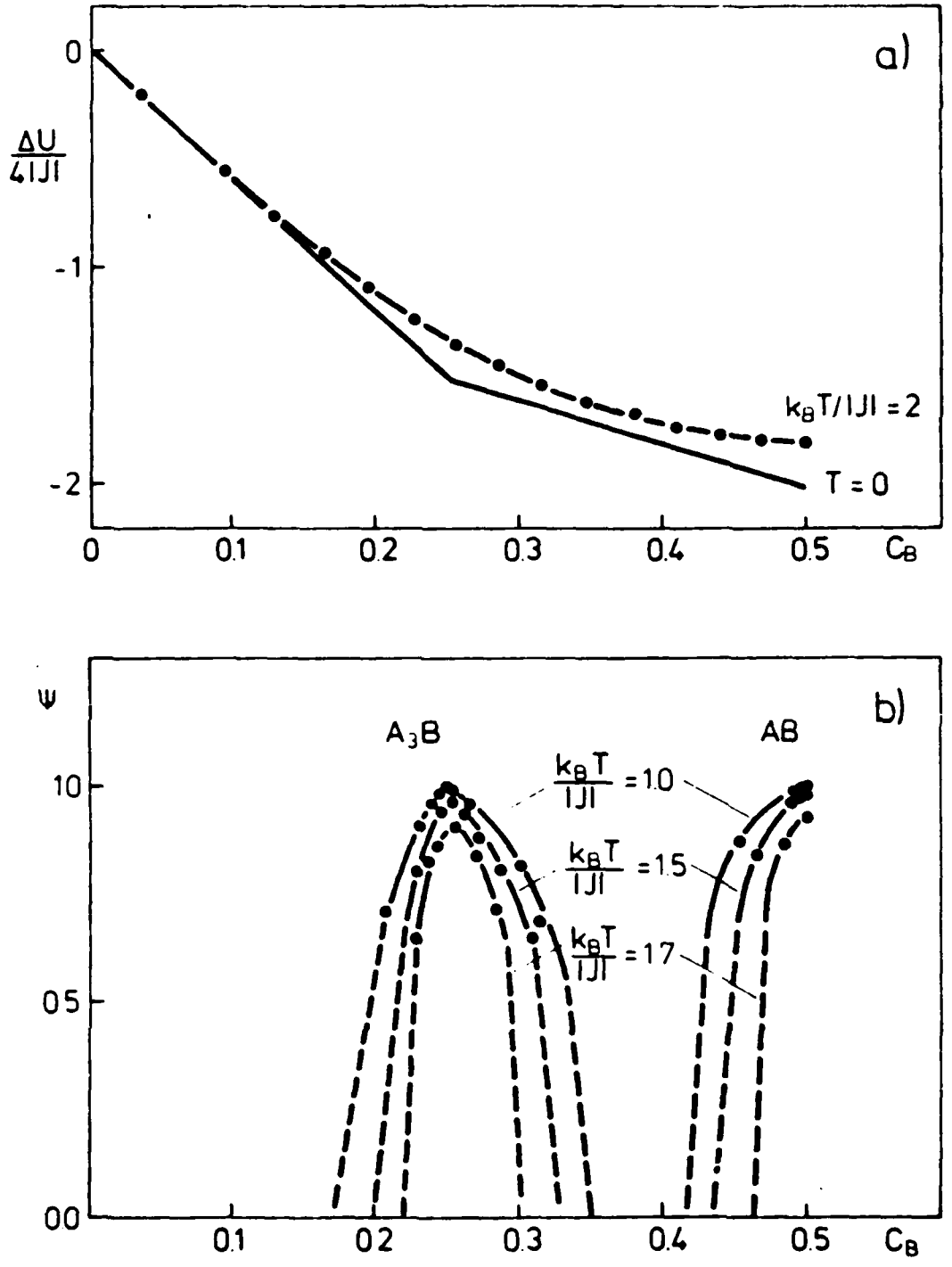
a)
0
-1
-2
ΔU/4|J|
0
0.1
0.2
0.3
0.4
0.5
C_B
$k_BT/|J| = 2$
T = 0
b)
Ψ
10
05
00
A_3B
AB
$\frac{k_BT}{|J|} = 1.0$
$\frac{k_BT}{|J|} = 1.5$
$\frac{k_BT}{|J|} = 1.7$
0.1
0.2
0.3
0.4
0.5
C_B

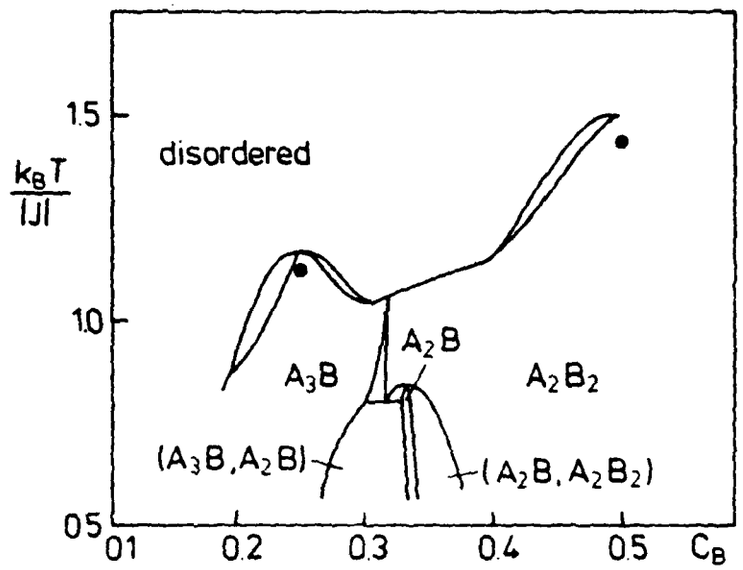
1.5
1.0
0.5
$\frac{k_B T}{|J|}$
disordered
A_3B
A_2B
A_2B_2
(A_3B, A_2B)
(A_2B, A_2B_2)
0.1
0.2
0.3
0.4
0.5
C_B